Human Gait Analysis by Body Segmentation and Center of Gravity

Ying-Fang Tsao*, Wen-Te Liu †and Ching-Te Chiu‡
*Department of Computer Science and Engineering, National Tsing Hua University, Hsinchu, Taiwan, R.O.C.
E-mail: s100062525@m100.nthu.edu.tw
†Taipei Medical University-Shuang Ho Hospital, Taipei, Taiwan, R.O.C.
E-mail: lion5835@gmail.com
‡Department of Electrical Engineering, National Tsing Hua University, Hsinchu, Taiwan, R.O.C.
E-mail: ctchiu@cs.nthu.edu.tw Tel: +886-3-5731208

***Abstract*—The physiological condition of a person may affect his/her daily behaviour such as gait or posture. For example under the fatigue condition, a person may be used to walk in a slower pace than usual. This paper presents a novel gait analysis approach to detect movement variations such as walking pace or speed change, walking with bending, walking with heavy breath, arm or leg swing change. Based on the geometry of the silhouette, we segment the body to five main parts including head, upper body, lower body, arms and legs. For a specific analysis, we segment the torso to upper and lower body. For the walking pace analysis, we use the leg movement in the lower body to find the max distance in a pace cycle and corresponding pace speed. The angles between the head or upper body and the vertical line are used to detect the walking with bending or walking with breathing. The arm swing angle or pace variation during walking can also be detected. We compare the normal condition with other abnormal condition such as people who have respiratory obstruction leading to heavy breathing, and have stomach ache resulting humpbacked status. These cause the angle of upper body different with normal condition, so we can observe these signals to give a warning notice. Our experiments show that with these fine posture features, we are able to detect a person's gait change. Examples are that a person is humpbacked, or the arm/leg swing and pace distance are in abnormal rhythm. From our gait analysis approach, we observe that when people are in a tired condition, they are used to adopt a static and comfortable pace distance to walk in our experimental results.**

I. Introduction

Gait analysis techniques help for the assessment of gait disorders and effects of disease such as chronic obstructive pulmonary disease (COPD). Patients with COPD are often asked to take around 10 minutes' walk before the breathing test. Research shows that the gait abnormalities in patients with COPD are present even when the subject is well rested. Fitness instructors, athletic coaches, physical therapists and orthopedic surgeons use gait and posture analysis as a means of determining susceptibility to injury. There are limited researches using video sequence to detect gait pattern change to assist doctors or therapists' diagnosis and treatment. We use the body segmentation approach as a base to extract the gait features. Previous studies on body segmentation are based on the methods of finding the geometry of the silhouette and using the color salience. Triangulations are used to construct the skeleton of a body [1]. Chellappa *et al.* segment the body by convex hull of the contour in the silhouette [2]. Nakamura *et al.* utilize the HMM model to construct the skeleton [3]. Fan *et al.* employ the body parts detection on colour image for segmentation [4]. Vision-based pace recognition or analysis is conducted in many studies [5], [6], [7]. Liu *et al.* present a simple method that aligns and averages the silhouettes over one pace cycle for pace recognition [5]. Han *et al.* uses the gait energy image as templates for the principle component analysis to recognize the pace [6]. The pace information is not only used in recognition biometrics, but also used in the detection of human physiological condition. Juang *et al.* apply the analysis on gait rhythm to Parkinson's disease [7]. Our proposed system utilizes segmentation to extract body parts. The center of gravity (COG) of the body parts such as head, upper and lower body, legs and arms, are used to analyze the movement and angle changes of human body and the gait rhythm. Taking the humpbacked or bending condition for example, we could utilize the angle of upper and lower body and the angle of the head and upper body to detect. When a person is tired or in a rush, the pace distance or the pace speed is different from the normal ones. We could use the swing of legs (pace rhythm) or arms to analyze pace distance and pace speed. Incorporating these fine features, we can detect the gait disorders for home care system applications [8], and human physiological condition detection.

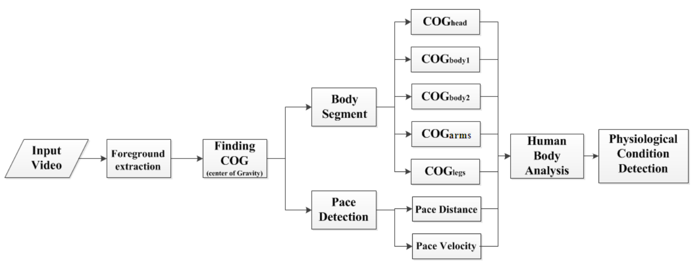

Fig. 1. The overall framework of Human Physiological Condition Detection System.

II. Feature-based Gait Analysis

The overall framework of our proposed gait analysis is shown in Fig. 1. Given an input video, we first extract the body silhouette by foreground extraction [9]. Then we find the center of gravity (COG) of the body silhouette. Next we use body segmentation to separate the body into five parts including head, upper body, lower body, arms and legs. Then we find the COG of each part. We utilize the relationship of each COG to determine the angle of bending and the angle of oscillating arms, and legs. We define a pace as the maximum moving distance of the leg in a cycle. Using the leg movement, we detect a pace and measure the pace distance in terms of pixels and pace velocity from the video frame rate. Combining these information, we analyze the detailed signals of the whole body and the pace distance to determine the normal, abnormal and uncomfortable condition of the people during walking.

A. Body Segmentation

We first use foreground extraction to obtain the human body silhouette as shown in Fig. 2(a). Then we find the center of gravity (COG) of the body silhouette (denoted as $Body_{(xi,yi)}$) by Eq.1.

$$(COG_x, COG_y) = \left(\frac{1}{N}\sum_{i=1}^{N} Body_{xi}, \frac{1}{N}\sum_{i=1}^{N} Body_{yi}\right), \quad (1)$$

N is the total number of pixels in the body silhouette. We find

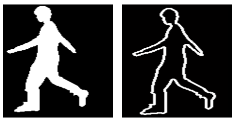

(a) (b)

Fig. 2. (a) Extracted Silhouette. (b) Extracted Contour.

the COG of the whole body denoted as $COG_{(x,y)}$. Then, we divide the top and bottom human body by a horizontal line passing through the $COG_{(x,y)}$ (the blue circle in the silhouette) as shown in Fig.3(a). We find another COG denoted as $COG_{v1(x,y)}$ for the top human body (the yellow part) in Fig. 3(b). A horizontal line passing through $COG_{v1(x,y)}$ is used to further divide the upper body into two parts. In the same way, we find the $COG_{v2(x,y)}$ of the upper part in the top human body as shown in Fig. 3(c). We utilize the Sobel Edge detection on the body silhouette to extract the contour as shown in Fig. 2(b). After finding the $COG_{(x,y)}$, $COG_{v1(x,y)}$, and $COG_{v2(x,y)}$,we draw the three distance maps called as DM_A, DM_B, and DM_C respectively by computing Euclidean distance between the contour and $COG_{(x,y)}$, $COG_{v1(x,y)}$ and $COG_{v2(x,y)}$ shown in Fig. 3(d), (e), and (f). We take the top point in the contour as the starting point to compute the distance map by Eq. 2.

$$DM_i = \sqrt{(COG_x - xi)^2 + (COG_y - yi)^2}, \quad (2)$$

$$(xi, yi) \in \textit{the position of the ith pixel in contour}$$

In the distance maps shown in Fig. 3(d), (e), and (f) clockwise finding by respective contour, the valley points are denoted using green triangular and peak points using red star. The corresponding points in the contour of the silhouette are shown in Fig. 3(a), (b), and (c). In order to segment the body into

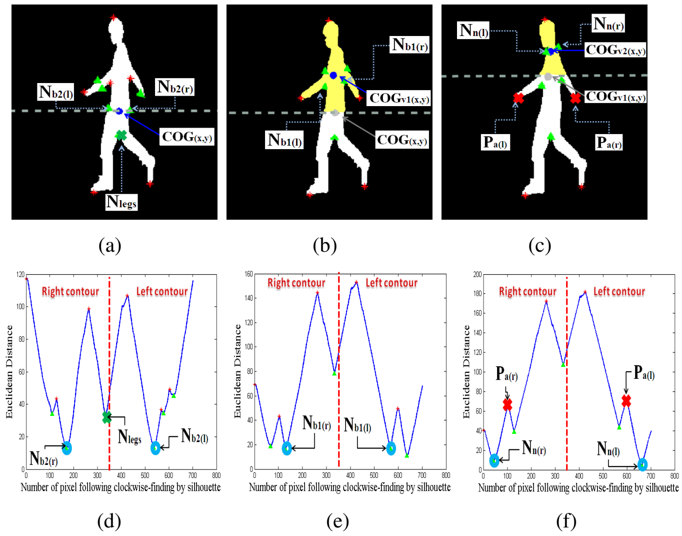

Fig. 3. (a) Finding $COG_{(x,y)}$ in silhouette. (b) Finding $COG_{v1(x,y)}$ in silhouette. (c) Finding $COG_{v2(x,y)}$ in silhouette. (d) The Distance Map of $COG_{(x,y)}$ and human contour denoted as DM_A. (e) The Distance Map of $COG_{v1(x,y)}$ and human contour denoted as DM_B. (f) The Distance Map of $COG_{v2(x,y)}$ and human contour denoted as DM_C.

head, upper body(body1), lower body(body2), arms, and legs as shown in Fig. 4(b), we use the distance map and the body contour to find the six lines for segmentation, denoted as L_n, L_{b1}, L_{b2}, L_{legs}, $L_{a(l)}$, and $L_{a(r)}$ shown in Fig. 4(a). Each line is determined by two valley points in the distance map. To find the line L_{b2} separating legs and human body, we use DM_A to search nodes with the minimum distance in right $N_{b2(r)}$ and left contour $N_{b2(l)}$ to the $COG_{(x,y)}$ as shown in Fig. 3(d). For the line L_{b1} separating the upper and lower body, we use DM_B to search the valley points $N_{b1(r)}$ and $N_{b1(l)}$ in right and left contour with COG_{v1}. For the line L_n, we use DM_C to search the valley points $N_{n(r)}$ and $N_{n(l)}$ with COG_{v2} in right and left contour shown in Fig. 3(f). We

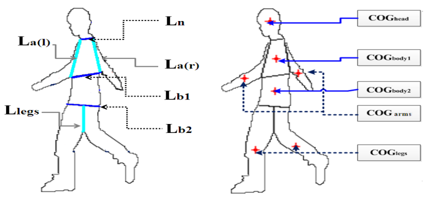

(a) (b)

Fig. 4. (a) Six cutting lines: L_n, L_{b1}, L_{b2}, L_{legs}, $L_{a(l)}$, and $L_{a(r)}$. (b) COG of the segmented parts.

use distance map DM_C to find the line $L_{a(r)}$ and $L_{a(l)}$ for segmenting the arms as shown in Fig. 4(a). First, we search the peak points in right contour in DM_C between the position of the $N_{n(r)}$ and $N_{b2(r)}$. When a peak point does not exist, we define that the person is in the close hand condition. If there exists a peak point shown in Fig. 3(c) and (f) denoted as $P_{n(r)}$, we connect the neighbour valley points of $P_{n(r)}$ to segment arms. Taking the right arm segmentation for example, we find the peak point in Fig. 3(f) with red cross in right contour. We connect its neighbour green valley points as $L_{a(r)}$. The line for segmenting the left arm is done in the same way. For segmenting legs, we use DM_A to find a line L_{legs} as shown in Fig. 4(a). We search a valley point between $N_{b2(r)}$ and $N_{b2(l)}$ as shown in Fig. 3(d). By connecting this valley point and the middle point in L_{b2}, we can build L_{legs}. When this valley point does not exit, we denote that the person is in the close leg condition. After finding these lines, we can segment the body into seven parts, head, body1, body2, left arm, right arm, left leg and right leg. Then we find the COGs of the segmented parts denoted as COG_{head}, COG_{body1}, COG_{body2}, $COG_{arm(l)}$, $COG_{arm(r)}$, $COG_{leg(l)}$, and $COG_{leg(r)}$ shown in Fig. 4(b). Using the relationship of the COGs, we determine the angle of bending and the angle of oscillating arms, and legs in Fig. 5(a). For the angle of bend-

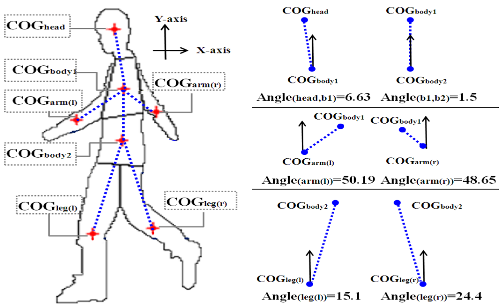

(a) (b)

Fig. 5. (a) Connecting the COGs. (b) The angles between the vectors and y-axis.

ing, we utilize Angle(head,b1) and Angle(b1,b2) shown in first row of Fig. 5(b). Denote vector(head,b1) as the line connecting COG_{head} and COG_{body1} and Angle(head,b1) is the angle between the vector(head,b1) and y-axis. The Angle(head,b1) can be used to detect the neck bending degree. Angle(b1,b2) is obtained by computing the angle between the vector(b1,b2) (the line connecting COG_{body1} and COG_{body2}) and y-axis. The Angle(b1,b2) is used to detect the vertebral bending degree. We utilize both these two angles to determine the angle of bending. For detecting right oscillating arms, we use the angle between the vector(arm(r),body1) (the line connecting $COG_{arm(r)}$ and COG_{body1}) and y-axis to determine the angle of Angle(arm(r)) shown in 2nd row of Fig. 5(b). Using the same way, we find the Angle(arm(l)). The Angle(leg(r)) is computed by the angle between the vector(leg(r),body2) (line connecting $COG_{leg(r)}$ and COG_{body2}) and y-axis shown in 3rd row of Fig. 5(b). The same way is used to find the angle in the left leg side.

B. Pace Feature Detection

Figure 6(a) shows the pace sequence in silhouette and Fig. 6(b) shows the mapped pace distance by pixel and the computed component in the leg part of the body. The component is computed by the L_{legs} shown in Fig. 4. If there exists L_{legs}, we determine that the legs has two separated part of the body. And we define it has two components. Otherwise, it only has one component. We define one pace as a cycle that changes from one component to two components then back to one component. Taking Fig. 6 for example, the first pace is from frame 2 to frame 15 and the second pace is from frame 16 to frame 27. The black line shows the walking distance of the current frame. The pace distance is defined as the maximum distance within a cycle. For example, the first pace distance is the maximum distance from the frame 2 to frame 15 and occurs around frame 7 with value of 60 pixels.

(a)

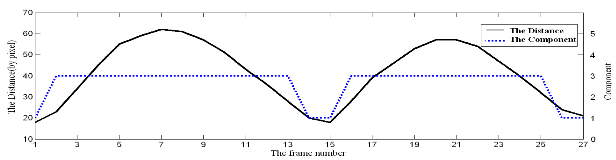

(b)

Fig. 6. (a) Pace sequence in silhouette(frame number:1,3,5,...). (b) The distance of each frame and the component of lower limbs.

III. Experimental Results

In this section, experimental results are reported to demonstrate the effectiveness of our proposed approach to detect of human physiological condition with side view captured by the camera.

A. The Characteristics of Angles when walking

To evaluate our proposed approach, we record the gait sequences of three people under three cases: normal walking, walking with bending and walking with heavy breathing. The tested person walks 30 meters for ten times for each gait sequence. Each gait sequence is about 10 minutes with 30 frames per second. When people are in their normal walking sequence, Angle(head,b1) and Angle(b1,b2) are supposed to be small as shown in Fig. 7(a). When a person bends himself during walk, the humpbacked condition is observed as shown in Fig. 7(b). When people walk with heavy breathing, they tend to bend themselves to complete the action of heavy breathing as shown in Fig. 7(c). We can use the Angle(head,b1) to determine a person's bending degree during walking. Table I shows the Angle(head,b1) of three people when they are in normal walking, walking with bending and walking with heavy breathing. For the gait sequence of walking with bending, the Angle(head,b1) has the largest values than other two

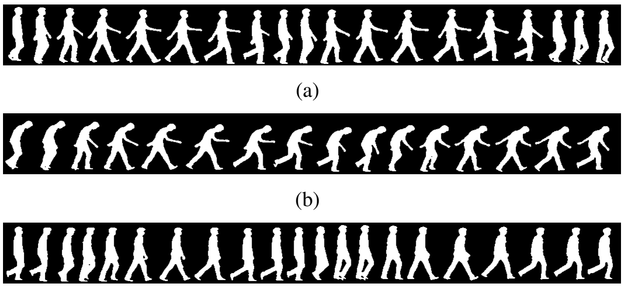

(a)

(b)

(c)

Fig. 7. (a) Walking sequence: the average of Angle(head,b1)=11.34, Angle(b1,b2)=4.08. (b) Walking with bending sequence: the average of Angle(head,b1)=51.26, Angle(b1,b2)=21.04. (c) Walking with heavy breathing sequence: the average of Angle(head,b1)=24.05, Angle(b1,b2)=6.79.

conditions. The Angle(head,b1) of the walking and walking with breathing are similar in some cases, because the breathing is not obvious in the sequence. We observe that the Angle(head,b1) in normal walking for Person 1 is larger than Person 2 and Person 3 in their normal walking, it is because person 1 bends a little in normal walking sequence. All things considered, if a person is bending, the Angle(head,b1) will exceed 4 times of the person who is walking. If the person has a heavy breathing, the Angle(head,b1) will be in the 2 to 4 times of the person who is walking. This analysis not also uses in the self-comparison, but also in the bending degree decision. If the Angle(head,b1) is over 10 degree, we thought that he or she has a little bending when walking. We can use it as a warning to tell the person that his/hers walking behaviour has to calibrate.

TABLE I
THE AVERAGE VALUE OF ANGLE(HEAD,B1) FOR THREE PEOPLE IN THREE POSTURES, WALKING, WALKING WITH BENDING, AND WALKING WITH HEAVY BREATHING.

Angle(head,b1)		walking	bending	walking with heavy breathing
Person 1	Average	10.145	57.24	30.96
Person 2	Average	5.18	30.42	15.15
Person 3	Average	6.7	34.07	10.07

B. The Characteristics of Physiological condition

We design another experiment for testing the pace variations under three scenarios. The object walks normally under the first scenario. The second case records the gait sequence right after the tested person runs for 30 minutes. The last case shoots the walking pattern right after the tested person running for 60 minutes. The same as the previous experiments, the tested person walks a length of 30 meter for ten times. Each gait sequence is about 10 minutes with 30 frames per second. For the above three cases, the tested object is supposed to be the most tired condition for scenario three since the object runs for the longest time than others. Figure 8 shows the thirty pace distance in the middle of the video under normal walking, walking after a short run, and walking after a long run.We find that the variance is the lowest in Fig. 8 with blue line, and this is under the condition when the person walks after a long run. Table II shows the average and variance of pace distance in walking, walking after a short run, and walking after a long run for Person 1 and Person 2. For the most fatigue

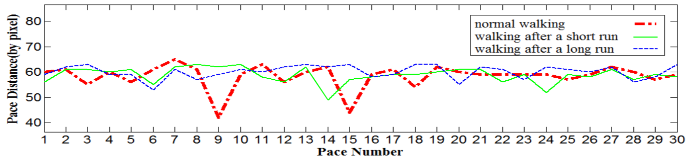

Fig. 8. The pace distance of Person 1 in normal walking, walking after a short run, and walking after a long run.

condition, the variances are the smallest for both persons. Also, the variances gradually decrease from normal walking to walking under tired condition. The more tired people are, the smaller variances of the pace distance are. It is because people tends to use a comfortable pace to walk when they are tired. By comparing the pace distance variance with that of normal walking, we could detect whether a person enters a static mode of walking. This can be used as a reference for doctors to tell a person's physiological condition, if we find the variance is less than previous and it is in the decreasing condition.

TABLE II
THE AVERAGE AND VARIANCE FOR TWO PEOPLE IN NORMAL WALKING, WALKING AFTER A SHORT RUN, AND WALKING AFTER A LONG RUN.

Pace Distance(pixel)		Walking in normal	Walking after a short run	Walking after a long run
Person 1	Average	58.48	58.86	60.16
	Variance	4.77	3.14	2.62
Person 2	Average	59.84	64.77	67.62
	Variance	3.73	3.4	2.54

IV. CONCLUSION

In our human gait analysis approach, we analyze the detailed signals of the whole body and the pace distance to determine the fine gait variation during walking. The proposed method utilizes the geometry of the silhouette to segment the body, and the movement of body legs to find the pace distance. Finding the COGs of the segmented components is valuable in representing the body information, because each COG is on the behalf of the segmented component. The changes of COG indicate the gait variation of the human.

REFERENCES

[1] J. W. Hsieh, C. H. Chuang, S. Y. Chen, and K. C. Fan, "Segmentation of Human Body Parts Using Deformable Triangulation," *IEEE TRANSACTIONS ON SYSTEMS, MAN, AND CYBERNETICSPART A: SYSTEMS AND HUMANS*, vol. 40, no. 3, pp. 596-610, May 2010.
[2] Zhanfeng Yue, and Rama Chellappa, "Synthesis of Silhouettes and Visual Hull Reconstruction for Articulated Humans," *IEEE TRANSACTIONS ON MULTIMEDIA*, vol. 10, no. 8, pp. 1565-1577, Dec. 2008.
[3] R. B. Lin and C. M. Tsai, "Online Segmentation and Clustering From Continuous Observation of Whole Body Motions," *IEEE TRANSACTIONS ON ROBOTICS*, vol. 25, no. 5, pp. 1158-1166, Oct. 2009.
[4] L. S. Hooi1, G. S. Liau, and C. Fan, "Human Pose Modelling and Body Tracking from Monocular Video Sequences," *International Conference on Intelligent and Advanced Systems*, pp. 571-576, 2007.
[5] Z. Liu and S. Sarkar, "Simplest Representation Yet for Gait Recognition: Averaged Silhouette," *Proc. IEEE Intl Conf. Pattern Recognition*, vol. 4, pp. 211-214, 2004.
[6] J. Han and B. Bhanu, "Statistical Feature Fusion for Gait-based Human Recognition," *Proc. IEEE Intl Conf. Computer Vision and Pattern Recognition*, vol. 2, pp. 842-847, 2004.
[7] Y. Wu, and S. Krishnan, "Statistical Analysis of Gait Rhythm in Patients With Parkinsons Disease," *IEEE TRANSACTIONS ON NEURAL SYSTEMS AND REHABILITATION ENGINEERING*, vol. 18, no. 2, pp. 150-158, April 2010.

[8] C. F. Juang, and C. M. Chang, "Human Body Posture Classification by a Neural Fuzzy Network and Home Care System Application," *IEEE TRANSACTIONS ON SYSTEMS, MAN, AND CYBERNETICSPART A: SYSTEMS AND HUMANS*, vol. 37, no. 6, pp. 984-991, Nov. 2007.

[9] H. Sekkati, R. Lagani'ere, A. Mitiche, and R. Youmaran, "Robust background subtraction using geodesic active contours in ICA subspace for video surveillance applications," *Ninth Conference on Computer and Robot Vision*, pp. 190-197, 2012.